ABACO-2: a comprehensive model for microalgae-bacteria consortia validated outdoor at pilot-scale

Rebecca Nordio[a,b], Enrique Rodríguez-Miranda[b,c], Francesca Casagli[d], Ana Sánchez-Zurano[a,b], José Luis Guzmán[b,c], Gabriel Acién [a,b]

[a] Department of Chemical Engineering, Universidad de Almería, E04120 Almería, Spain.

[b] CIESOL Solar Energy Research Centre, Joint Centre University of Almería-CIEMAT, 04120 Almería, Spain.

[c] Department of Informatics, Universidad de Almería, E04120 Almería, Spain.

[d] Biocore, INRIA centre d'Université Côte d'Azur, Sophia-Antipolis F-06902, France.

[*] **Corresponding author:** Rebecca Nordio, rnordio@ual.es

Abstract

Modelling microalgae-bacteria in wastewater treatment systems has gained significant attention in the last few years. In this study, we present an enhanced version of the ABACO model, named ABACO-2, which demonstrates improved accuracy through validation in outdoor pilot-scale systems. ABACO-2 enables the comprehensive characterization of microalgae-bacteria consortia dynamics, allowing to predict the biomass concentration (microalgae, heterotrophic bacteria, and nitrifying bacteria) and nutrient evolution. The updated version of the model incorporates new equations for nutrient coefficient yields, oxygen mass balance, and microorganism cellular decay, while significantly reducing the number of calibrated parameters, simplifying the parameter identification. Calibration and validation were performed using data from a 80 m^2 raceway reactor operated in a semicontinuous mode over an extensive period (May to November, total of 206 days) at a fixed dilution rate of 0.2 day^{-1} (corresponding to 5 days of hydraulic retention time), where untreated urban wastewater was used as culture medium. ABACO-2 exhibited robustness, accurately forecasting biomass production, population dynamics, nutrient recovery, and prevailing culture conditions across a wide range of environmental and water composition conditions. Mathematical models are essential instruments for the industrial development and optimization of microalgae-related wastewater treatment processes, thereby contributing to the sustainability of the wastewater treatment industry.

KEYWORDS: Microalgae, wastewater, modeling

1. Introduction

Water reuse and recycling have become crucial topics of discussion in recent decades, owing to their significant environmental and social implications. With rapid industrialization and population growth, the volume of wastewater generated annually has escalated (Angelakis and Gikas, 2014). contributing to water stress in various regions worldwide, particularly in southern Europe, including Spain, Italy, and Greece (Strosser et al., 2012). Consequently, researchers have directed their efforts toward developing innovative water remediation technologies. Among these technologies, microalgae-based wastewater systems have emerged as a promising solution, capable of replacing traditional secondary and tertiary classical wastewater treatment processes (Abdel-Raouf et al., 2012). The utilization of microalgae in water remediation offers several advantages. Firstly, it demands less energy compared to conventional methods. Secondly, it significantly reduces greenhouse gas emissions. Additionally, microalgae systems eliminate residues effectively and yield valuable biomass, which can be utilized in various industrial applications (Mohd Udaiyappan et al., 2017).

Microalgae are photosynthetic microorganisms capable of using CO_2 as a carbon source and light as an energy source, in addition to using nitrogen (N) and phosphorus (P) present in wastewater to produce biomass. Moreover, thanks to the presence of bacteria, the organic matter's degradation is ensured (Muñoz and Guieysse, 2006). The effectiveness of microalgae-based wastewater systems has been demonstrated through pilot-scale testing in raceway reactors (Morillas-España et al., 2021b) and thin layers (Grivalský et al., 2019). These studies have proven that these systems are robust and reliable, enabling the recovery of nutrients from wastewater and producing treated water that meets the regulatory standards set by European legislation (Council Directive of May 1991 concerning urban wastewater treatment, 1991). One of the key factors contributing to the success of this technology is its resilience in the face of significant variations in water composition and weather conditions (Nordio et al., 2023). However, high costs and relatively low efficiency are foreclosing the entire industrial development of these systems (Acién et al., 2014). The industrial development of these processes can be possible only after the improved understanding and

optimized management of the biological system allowing to study which are the main parameters influencing biomass productivity and the water remediation capacity (Solimeno and García, 2017).

In this framework, mathematical modelling serves as a valuable tool for describing these processes; as it enables simulations and performance evaluations under different environmental and process conditions, aiding optimization and the development of control strategies (Solimeno and García, 2017). In the literature, it is possible to find many examples of microalgae models that evaluate the growth rate as a function mainly of light, temperature, nutrients and pH (Lee et al., 2015). On the contrary, a few examples of comprehensive models for microalgae-based wastewater treatments are available, defined as models that consider the effect of multiple process parameters and biological mechanisms. Examples of recent comprehensive models are the Zambrano model (Zambrano et al., 2016), the BIOALGAE model (Solimeno et al., 2019), and the ALBA model (Casagli et al., 2021). Nevertheless, it is challenging to obtain validation data over an extended period and using urban wastewater in industrial facilities, so in the literature, some alternatives can be found, such as validations achieved with digestates, synthetic waters, or small-scale reactors. However, it is crucial to develop models that accurately represent the biological system in real conditions (both environmental and operational) since they are intended for use in commercial wastewater treatment facilities. In Spain, for example, there are currently four industrial facilities using microalgae for urban wastewater treatment, employing reactors ranging from 0.5 to 1.0 ha (Masojídek et al., 2022).

To apply these models to large-scale production, it is important to balance complexity and realism. For instance, very complex mathematical descriptions of all the metabolic reactions involved in photosynthesis, may not improve the model prediction accuracy, compared to the computational cost required. Additionally, mechanisms that are not relevant for long-time series and continuous conditions can be omitted from the model (Darvehei et al., 2018). Furthermore, in wastewater, thousands of bacterial groups can interact with microalgae, and it is fundamental to carefully select the most relevant groups to reduce the number of equations and the overall complexity. Generally, only a few groups are considered relevant, as they influence nutrient uptake from the culture medium. The first model was proposed by Buhr & Miller in 1983 (Buhr and Miller, 1983), for example,

only two populations (algae and aerobic bacteria) were considered. However, afterwards, the leading bacterial groups identified were the heterotrophic bacteria, which permitted the oxidation of the organic matter, and nitrifying bacteria that compete with microalgae for the consumption of nitrogen (together with phosporous and carbon) in some cases distinguished between ammonia-oxidizing bacteria (AOB) and nitrite-oxidizing bacteria (NOB) (Aparicio et al., 2022a).

In this work, an improved version of the ABACO model (Sánchez-zurano et al., 2021), named the ABACO-2 model is proposed, calibrated and validated for outdoor conditions. The original ABACO model is a recent microalgae-bacteria model designed to represent the dynamics of these populations in wastewater systems. This model underwent validation over three weeks using a 1L tubular reactor, fed with various types of wastewaters. While it served as a valid foundation for subsequent modeling research, further improvements were necessary to validate it at the pilot-scale level. Specifically, new equations are included to reduce the number of calibrated parameters, and the use of the oxygen mass balance allows for improvement in the accuracy of the model. Equations have been implemented using Python language and numpy packages while the calibration has been carried out with Scipy library and the optimization tool that uses the "Nelder-Mead" algorithm. The model has been validated over an extensive period (May-November); data have been collected from a demonstrative pilot-scale raceway reactor of 12 m^3 (80 m^2) on which the prevailing strain was *Scenedesmus sp.*. The reactor was operated in semi-continuous mode at a fixed rate of 0.2 day^{-1} using urban wastewater as culture medium. For this study, wastewater not pre-treated besides the removal of large particles was used, so subjected to high variation in terms of composition. This large variability of water nutrient concentration, together with different values of solar radiation and temperature typical of different year seasons, allowed to calibrate and validate the model in a wide range of conditions (Section 2.2), so increasing its prediction accuracy and robustness.

2. Material and methods

2.1. Raceway reactor and inoculum

Experimental data were collected from an 80 m^2 (12 m^3) raceway reactor working in semi-continuous mode between April and December, with a fixed dilution rate (reverse of the hydraulic retention time

time) of 0.2 day^{-1}, meaning that every day a 20% of the total volume of the culture have been removed and replaced with wastewater. The raceway was installed in the SABANA Demo Plant located in the IFAPA research centre in La Cañada, Almería, Spain. It was composed of a double channel of 40 m and a sump of 0.59 m^3 for the gas injections through diffusers and an electric motor connected to a paddlewheel system for culture mixing. The pH was monitored through sensors and controlled through CO_2 injection in the reactor sump. Additionally, an independent airflow allowed reducing the concentration of dissolved oxygen. The culture depth was fixed at 0.15 m. In order to thoroughly monitor the culture dynamics, additional sensors have been installed for recording the dissolved oxygen (0-400% Sat), pH (0-14), temperature (0-80°C) and culture depth (4-40 cm). Moreover, a meteorological station allowed for registering the weather conditions regarding solar radiation and environmental temperature.

The chosen inoculum was *Scenedemus sp.* because it was demonstrated to be suitable microalgae that can easily be grown in wastewater and a wide range of conditions (Fernández Sevilla et al., 2006). The strain was initially grown on a fertilizer medium (0.9 $g \cdot L^{-1}$ of $NaNO_3$, 0.18 $g \cdot L^{-1}$ of $MgSO_4$, 0.14 $g \cdot L^{-1}$ of KH_2PO_4 and 0.003 $g \cdot L^{-1}$ of Kerantol), first using columns of 0.1 m^3 and then in a tubular system of 3 m^3 until it reached the concentration of 1 $g \bullet L^{-1}$. The biomass was then used as inoculum for the raceways. The culture was diluted with wastewater and kept in batch mode for one week, after that being operated in semi-continuous mode until it reached a stable biomass concentration (approximating a steady state condition).

2.2. Environmental conditions and water composition

As previously mentioned, environmental conditions in terms of temperature and radiation were continuously recorded throughout the entire period. The Photosynthetically Active Radiation (PAR) registered were ranged from 2000 $\mu E \cdot m^{-2} \cdot s^{-1}$ during the months of April and May, gradually decreasing during the colder seasons with peaks at 1200 $\mu E \cdot m^{-2} \cdot s^{-1}$, with an average of 620 $\mu E \cdot m^{-2} \cdot s^{-1}$ and 350 $\mu E \cdot m^{-2} \cdot s^{-1}$respectevely. Regarding temperature, the highest values were recorded during the summer season (July-August), reaching peaks of 38°C, while in the spring season (April-

May), they ranged between 25-35 °C, and in the autumn season (September-November), between 25-12 °C.

Regarding the culture medium, it consisted of wastewater collected from the University of Almería during the entire data collection period, except for August when the water was sourced from the primary water treatment plant in the city of Almeria. In both instances, the water underwent pre-treatment, involving the removal of solid particles through an industrial filter (Azud Helix, 200 µm), before being introduced into the culture. During the study period, the nutrient concentration of the wastewater varied over a wide range. Specifically, ammonium (NH_4^+) concentration varies between 10 - 400 $g•m^{-3}$, nitrate (NO_3^-) concentration ranged from 0- 13 $g•m^{-3}$, phosphate (PO_4^{2-}) between 30 - 76 $g•m^{-3}$, while the chemical oxygen demand (COD) between 100 – 600 $gO_2•m^{-3}$.

2.3. Biomass concentration and nutrients analysis

The influent wastewater and the filtered effluent were analysed in terms of nutrient content ($N\text{-}NO_3^-$, $N\text{-}NH_4^+$, $P\text{-}PO_4^{3-}$) and COD. The biomass concentration in the culture was daily measured through the dry weight (DW) method. The culture was collected in the morning after the reactor sump, and 100 mL were filtered in a 0.5 µm filter and let dry for 24h at 80°C in an oven. Regarding the nutrients, they were analysed through colourimetric methodologies in a spectrophotometer according to standard procedures (Standard IC 74246, Standard IC 38364, Standard IC 59755). The total COD was measured with Hanch-Lange kits (LCI-400) and the biodegradable soluble organic matter (BSMO) was estimated as a percentage of the total COD as reported in the literature by Pasztor I. et al., 2009.

2.4. Data collection and analysis

Experimental online data were collected every second by a set of sensors, connected to a Programming Logic Controller (PLC) and a Supervisory Control and Data Acquisition (SCADA) system. On the contrary, data coming from laboratory analysis as described in the previous section, were collected once a day. Given the big amount of data available, it was necessary to perform a prior data analysis following a procedure inspired by the “Cross Industry Standard Process Alliance

for Data Mining" (CRISP-DM) approach (Ncr and Clinton, 1999). This methodology is one of the most used among data mining problems and it is composed of six main steps: (i) Business understanding, (ii) Data understanding, (iii) Data preparation, (iv) Modelling, (v) Evaluation, and (vi) Deployment. In this research, the first five steps have been developed as briefly described below:

I. Business understanding: the objective is to develop a model that can describe the evolution of microalgae-bacteria populations in wastewater-related systems. The aim is to develop a tool that allows the simulation of the variation of biomass and nutrient concentration with time as a function of environmental and process parameters.

II. Data understanding: data have been collected as described in the previous section, studied, and analysed.

III. Data preparation: Datasets have been ordered, cleaned, and prepared for the modelling step.

IV. Modelling: the biological system has been modelled as described in the next sections. Stepping back to data preparation is often necessary. A part of the experimental data set has been used for the identification of the calibration parameters.

V. Evaluation: the developed model has been validated with long-term outdoor dataset. If the quality of the model was not enough to reach the defined objective, the data preparation and modelling part has been reviewed.

VI. Deployment: this step was not addressed in this research. However, a web interface for model utilization will be developed in future works.

3. Model development

3.1. Model concept

This work considers three microbial groups: microalgae, heterotrophic bacteria and nitrifying bacteria as they are the main actors in the nutrient uptake and the O_2/CO_2 fluxes (Figure 1). During the day, microalgae perform photosynthesis consuming the inorganic carbon and fixing nitrogen and phosphorus while producing O_2. The preferred nitrogen form for microalgae growth is NH_4^+, which is highly present in urban wastewater. Microalgae compete with nitrifying bacteria for the uptake of this compound since they use it to transform it into NO_3^- during the nitrification. The nitrification process

194 involved the oxidation of NH_4^+ to NO_2^- by AOB and then NOB transform NO_2^- into NO_3^-. For this
195 study, it is considered that the nitrification is complete because it was not registered a significant
196 concentration of NO_2^- in the culture (consistently below 5 g•m^{-3}). Moreover, microalgae can use NO_3^-
197 as a form of nitrogen, but its consumption takes place only when ammonium is found below a given
198 threshold (prior experimental analysis have estimated it as 80 g•m^{-3}). Heterotrophic bacteria are
199 considered the leading bacteria group as they are the main ones responsible for the degradation of
200 organic matter. For the present work, the COD has been fractionated as proposed by Pasztor I. et
201 al., 2009. Briefly, the total COD can be divided into two main fractions: the biodegradable (readily
202 and slowly) and the non-biodegradable (soluble and particulate). Heterotrophic bacteria can
203 consume only the readily biodegradable organic matter estimated as 22% of the total COD and it
204 will be called BSMO (biodegradable soluble organic matter), as proposed by the same authors.
205 Summarizing, the BSMO concentration is decreased in the culture due to the heterotroph's activity
206 and it can be increased due to the cellular death and decay of the microorganisms present in the
207 culture. Regarding the gas fluxes, the inorganic carbon necessary for microalgae growth is partially
208 provided by the on-demand injection of CO_2 for pH control and the natural release of CO_2 given by
209 bacteria during respiration. This study assumes that microalgae are never limited by inorganic
210 carbon concentration, as CO_2 injection always ensures enough carbon availability for microalgal
211 growth, as already demonstrated by previous studies (Posadas et al., 2015). Additionally,
212 experimental data performed into the system indicate that the liquid bulk alkalinity into the medium
213 is never exhausted, preventing the loss of injected CO_2 used for pH control. On the contrary, the O_2
214 is produced during photosynthesis by microalgae and used by bacteria for their respiration, and it is
215 partially removed from the culture broth due to mass transfer phenomena, mainly aeration into the
216 sump installed on the reactor.

217 ***Main changes implemented from ABACO model***

218 Despite the ABACO model served as the starting point for the development of ABACO-2, significant
219 modifications have been implemented to enhance prediction accuracy and process understanding.
220 Indeed, the ABACO model proposed by Sánchez-zurano et al., 2021, can be considered a

preliminary study, conducted with a limited expertise regarding microalgae cultivation phenomena. Furthermore, this model was developed using a restricted dataset and calibrated using data from laboratory-scale experiments conducted under controlled conditions. In contrast, with ABACO-2, the intention is to calibrate parameters under industrial conditions, utilizing a more extensive dataset that encompasses diverse operational and climatic scenarios.

The foremost modification involved the integration of models to account for cell death and respiration, coupled with the variation in BSMO content within the culture, subsequently reduced by heterotrophic bacterial activity. This refinement also led to a reduction in the number of parameters necessitating calibration. As an additional parameter reduction strategy, it was assumed that phosphate consumption by bacteria is minimal and primarily relevant for microalgae. Consequently, phosphate consumption yields for these microorganisms were excluded from the calibration set. Regarding nutrient yields, equations were introduced to describe the dynamics of nutrient uptake by algae as a function of their concentration in the medium. In this context, process rates were adjusted to consider that NO_3 consumption by algae is significant only when NH_4 levels are substantially reduced. Furthermore, in relation to nutrients, a correction parameter was incorporated into the Monod equations to account for nutrient accumulation by microalgae, preventing zero growth in such scenarios. In the context of refining the calibration process, parameters associated with nutrient consumption by bacteria (originally calibrated) were set and adopted from the Activated Sludge Models (ASM), and an oxygen balance was introduced. The O_2 concentration is a continuous measuremet within the reactor and it significantly facilitated parameter recognition during the calibration process. Finally, the parameters of the cardinal temperature equations were adjusted using those proposed by Casagli et al., 2021, as they are more representative, having been calibrated while considering winter seasons.

3.2. Model components

This section summarizes the main model components:

- S_{NH4} [$g_{NH4} \cdot m^{-3}$]: ammonium. It is present in the influent, and it is consumed especially by microalgae and nitrifying bacteria and in a lower amount by heterotrophic bacteria.

- S_{NO3} [g_{NO3}•m^{-3}]: nitrate. This form of nitrogen is generally null in the influent, but it is generated by the nitrifying bacteria during the nitrification process. Nitrate is consumed by microalgae when ammonium concentration in the medium is low.
- S_{PO4} [g_{PO4}•m^{-3}]: phosphate. Phosphorus is present as a dissolved component in the water inlet. Its consumption is mainly due to the activity of microalgae, while the uptake from bacteria is considered negligible.
- S_{BSMO} [g_{BSMO}•m^{-3}]: biodegradable soluble organic matter. This is a fraction of the total COD, assumed as 22%. It is consumed by heterotrophic bacteria and generated during the cellular decay of both microalgae and bacteria.
- S_{O2} [g_{O2}•m^{-3}]: dissolved oxygen. Oxygen is produced by microalgae during photosynthesis and consumed by microalgal respiration and by the activity of both bacterial populations. Moreover, the dissolved oxygen can be stripped to the atmosphere by bubbling air into the reactor sump.
- X_{alg} [g_{alg}•m^{-3}]: microalgae biomass. Microalgae proliferate starting from an initial inoculum, thus microalgae biomass is produced by fixing nitrogen and phosphorus, also consuming CO_2 while producing oxygen. Microalgae concentration in the inlet wastewater is considered negligible, while a given amount is harvested every day. Moreover, their growth decreases due to cellular death.
- X_{nit} [g_{nit}•m^{-3}]: nitrifying bacteria biomass. Nitrifying bacteria proliferate starting from an initial inoculum by consuming nitrogen in the form of ammonium and releasing nitrate. It is assumed that their concentration entering the system is negligible, while a given concentration is exiting during the harvesting. Moreover, their growth decreases due to cellular death.
- X_{het} [g_{het}•m^{-3}]: heterotrophic bacteria biomass. Heterotrophic bacteria proliferate starting from an initial inoculum by consuming the BSMO and nitrogen in the form of ammonium. It is assumed that their concentration entering the system is negligible, while a given concentration is exiting during the harvesting. Moreover, their growth decreases due to cellular death.

3.3. Boundary conditions

Concentrations must be always positive or equal to zero. This boundary condition can be expressed as in equation (1): when a concentration is approaching zero (assuming ε in the order of 10^{-8}), its derivative has to be equal or more than zero, meaning that it cannot generate negative matters.

$$if \quad X_i \leq \varepsilon \quad \rightarrow \quad \dot{X}_i\big|_{Xi=0} \geq 0 \qquad (1)$$

As a result, all the balances implemented for this model have been implemented according to equation (2), guaranteeing the boundary conditions to be satisfied.

$$\dot{X} = f(x,y) \cdot \frac{X}{X+\varepsilon} \qquad (2)$$

3.4. Biological processes

Table 1 summarizes the processes taken into consideration of the microalgae and the bacterial growth, while Table 2 is the relative matrix of the stoichiometric parameters. The mass balances for the microorganism's growth have been built according to equation (3):

$$Inlet - Outlet + Reaction = Accumulation \qquad (3)$$

where the *Inlet* and *Outlet* are the flowrates in [m^{-3}•s^{-1}] in and out of the system, generically defined as (4) and (5):

$$Inlet = Q_d X_{in} \qquad (4)$$

$$Outlet = Q_h X_{out} \qquad (5)$$

where Q_d is the dilution flow rate in [m^{-3}•s^{-1}], Q_h is the harvesting flow rate in [m^{-3}•s^{-1}], X_{in}/ X_{out} (or S_i/ S_{out}) is the concentration of component inlet or outlet in [g•m^{-3}].

The reaction (r_i, [g•m^{-3}•day^{-1}]) term can be obtained by summing the product of the yield coefficients, *vi* (Tables 2 and 5) and the process rate, ρ_j, as described in (6) (Henze et al., 2000)

$$r_i = \sum_i v_{i,j} \rho_j \qquad (6)$$

In summary, the processes considered in the ABACO-2 model are:

- ρ_1: microalgae growth in NH_4^+. Microalgae grow photosynthetically using NH_4^+ as a nutrient source, and contemporarily consuming PO_4^{3+} and CO_2 while producing O_2.
- ρ_2: microalgae growth in NO_3^-. Microalgae grow photosynthetically using NO_3^- as a nutrient source, and contemporarily consuming PO_4^{3+} and CO_2 while producing O_2. The growth in this nitrogen source is activated only once the medium is decreasing in NH_4^+ concentration.
- ρ_3: microalgae decay. This process includes both the algal biomass loss (decay), increasing the BSMO concentration in the medium, and the algal respiration that leads to a consumption of oxygen all over the entire process.
- ρ_4: nitrifying bacteria growth. Nitrifying bacteria growth consumes NH_4^+ and O_2 and produces NO_3^-.
- ρ_5: nitrifying bacteria decay. Bacterial biomass loss due to their decay; it leads to an increase in the BSMO concentration.
- ρ_6: heterotrophic bacteria growth. Heterotrophic bacteria growth consuming the BSMO, O_2 and NH_4^+.
- ρ_7: heterotrophic decay. Bacterial biomass loss due to their decay (it leads to an increase in the BSMO concentration).

3.4.1. Photosynthesis and respiration

The growth rate as a function of light was modelled using the equation proposed by Molina (Grima et al., 1994), as described in equation (7), where I_k in [$\mu E \cdot m^{-2} \cdot s^{-1}$] is the irradiance constant that represents the equivalent irradiance necessary to reach half of the maximal growth rate, *n* is the shape constant and I_{av} is the average light inside the reactor in [$\mu E \cdot m^{-2} \cdot s^{-1}$].

$$\mu(I_{av}) = \frac{{I_{av}}^n}{{I_k}^n + {I_{av}}^n} \quad (7)$$

The average light inside the culture was expressed following equation (8), and it depends on the incident light I_0 [$\mu E \cdot m^{-2} \cdot s^{-1}$], the extinction coefficient K_a [$m^2 \cdot g^{-1}$], the algal biomass concentration (X_{alg}) in [$g \cdot m^{-3}$] and the culture depth h [m].

$$I_{av} = \frac{I_0}{K_a X_{alg} h}\left(1 - \exp\left(-K_a X_{alg} h\right)\right) \quad (8)$$

Moreover, the average light was used to express the microalgal endogenous respiration as given by equation (9); where m_{max} and m_{min} are the maximum and the minimum respiration in [day^{-1}], I_{kr} is the irradiance necessary to stop photosynthesis and let begin the respiration and n_r is the shape form for respiration.

$$m_{alg} = m_{min} + \frac{m_{max}\ {I_{av}}^{n_r}}{{I_{kr}}^{n_r} + {I_{av}}^{n_r}} \quad (9)$$

Finally, bacterial decay has been taken into consideration as a constant effect during the cultivation process. m_{nit} and m_{het} [day^{-1}] have been modelled as a percentage of the maximum growth rate (as summarized in Table 4) corrected by a coefficient dependent on the temperature θ, as described in equation (10).

$$\theta = \theta_i(T - 20°C) \quad (10)$$

Where θ_i are specific parameters that depend on the bacterial population considered (Table 3).

3.4.2. Influence of pH, temperature, dissolved oxygen and nutrients

As described in Table 1, for each microorganism, the growth rate depends on a maximum specific growth rate μ value multiplied by a series of normalized factors that depends on the culture conditions of temperature, pH, O_2 and nutrient concentration. The growth rates of microalgae exhibit a bell-shaped function in response to temperature and pH. Initially, as temperature (or pH) increases from low values, the growth rate rapidly increases until it reaches its maximum, corresponding to the optimal parameter value. However, beyond the optimum, the growth rate decreases sharply with further increases in temperature (or pH). The pH parameters, minimum, maximum, and optimal values, were determined through laboratory measurements using the photo-respirometric method (Sánchez Zurano et al., 2021); Notably, bacterial parameters vary from those of microalgae, as their growth is favoured by higher values of pH (Table 4). In contrast, temperature parameters were

derived from previous modeling studies (Casagli et al., 2021), with the optimal temperature aligning closely with that of microalgae.

The growth dependence can be described through a cardinal equation with inflexion, developed for the first time by Bernard et alt. (Bernard and Rémond, 2012) (11). Similarly, the model proposed by Ippoliti et al. was used to describe the pH dependence (Ippoliti et al., 2016) (12).

$$\overline{\mu\,(T)} = \frac{(T - T_{max})(T - T_{min})^2}{(T_{opt} - T_{min})\left[(T_{opt} - T_{min})(T - T_{opt}) - (T_{opt} - T_{max})(T_{opt} + T_{min} - 2T)\right]} \quad (11)$$

$$\overline{\mu(pH)} = \frac{(pH - pH_{min})(pH - pH_{max})^2}{(pH_{opt} - pH_{min})\left[(pH_{opt} - pH_{min})(pH - pH_{opt}) - (pH_{opt} - pH_{max})(pH_{opt} + pH_{min} - 2pH)\right]} \quad (12)$$

Regarding the effect of dissolved oxygen, it is known that high concentrations are inhibitory for microalgal photosynthesis. According to previous studies on *Scenedemsus sp.*, the growth rate can be reduced by 25% when the concentration is increased up to 150% Sat, while below 250% Sat the photosynthesis is completely stopped. This effect was modelled using the equation proposed by Costache et al., 2013 and reported in equation (13). On the contrary, oxygen has been modelled as a nutrient source for bacteria growth, as described below.

$$\overline{\mu(O_2)_{alg}} = 1 - \left(\frac{S_{O_2}}{S_{O_2,max}}\right)^z \quad (13)$$

Finally, the influence of nutrient concentration on the growth rate was taken into account. As mentioned, nitrogen is a fundamental macronutrient that must be provided to microalgae to ensure their growth. The inorganic nitrogen can be assimilated into acids for the protein formations in many forms, such as NH^+_4, NO^-_2 and NO^-_3. However, in this study, the main nitrogen form present in wastewater was ammonium, while nitrate was formed only after the complete nitrification process. Ammonium is the favoured nitrogen form for microalgae as it requires less energy to be assimilated. Only after a given concentration threshold do microalgae begin to consume NO_3, which will be transformed into NH_4 to be assimilated into the cells. Phosphate is another fundamental macronutrient for microalgal growth, as it is necessary for the synthesis of RNA into the nucleotides, while it is assumed that this component is not consumed by bacteria. The growth rate as a function

of the substrate concentration, has been modelled using the Monod equation, as described in (14), (Monod, 1949)

$$\overline{\mu(S_i)} = \frac{S_i}{S_i + K_s} \quad (14)$$

The Monod equations for the nitrogen and the phosphorus for the process n.1 and 2 in Table 1 have been modified by the inclusion of a correction factor. With this modification, zero-growth when no longer nitrogen/phosphate are present in the medium was avoided. Indeed, it is already known that microalgae can store nutrients in cells guaranteeing their survival and growth even when the medium is limited in nutrients. This fact can be represented by more complex models such as the Droop model (Droop, 1970), which considers the cells quota of the limiting element. However, quotas are difficult to be estimated as they required specific laboratory techniques. For this reason, in this work, a simplified description of this phenomenon was chosen by correcting the concentrations in the Monod equation as the sum of the component available in the medium and the one present in the algal biomass (equal to 10% in nitrogen and 2% in phosphorus, multiplied by the "assimilation" factor α) (14), (15).

$$S_N = S_{N,medium} + X_{alg} * 0.1 * \alpha \quad (15)$$

$$S_P = S_{P,medium} + X_{alg} * 0.02 * \alpha \quad (16)$$

The kinetic parameters used for the Monod equation are summarized in Table 3.

3.4.3. Nutrient yields

Nutrient yield can be defined as the amount of nutrients consumed from the medium per gram of biomass produced. In the literature, it can be found that the nutrient yield for algae is not constant, but changes depending on the nutrient amount present in the medium. More specifically, it was found that the nutrient uptake rate is higher at lower nutrient concentrations until it is reached a maximum. This can be explained by some biological mechanisms like the "luxury uptake" (Solovchenko et al., 2019): microalgae store a larger amount of nutrients than the ones necessary for immediate growth. It is possible to suppose that nutrients yield not only depends on the nutrient concentrations in the

medium but even on environmental conditions and process parameters. However, modelling this phenomenon is complex, and in the literature can be found different results that mainly depend on the strain used and the type of experiment performed. The equations developed by Zurano et al., 2021 were taken as a good approximation of ammonium and phosphorus consumption rates by microalgae, as described in equation (17), where S is the substrate consumed by microalgae (NH_4^+, NO_3^- or PO_4^{-3}). This was developed as a combination between and hyperbolic and a cardinal equation. The hyperbolic equation, typically employed for describing microbial growth kinetics, helps explain the increase in nitrogen and phosphorous coefficient yields with higher nitrogen or phosphorous concentrations in the medium. Furthermore, to account for the observed peaks in both nitrogen and phosphorous coefficient yields, the cardinal equation has been applied within predefined minimum and maximum ranges. The cardinal model enables the definition of maximum, minimum, and optimal conditions for any variable, and it characterizes the influence of these variables on the biological system's performance as a Gaussian function. All the parameters values are summarized in Table 5.

$$Y_{s,alg} = \left[\frac{Y_{max}\ S^{t_S}}{{S_N}^{t_s}\ {K_{s,Y_s}}^{t_S}}\right] + \left[\frac{(S - S_{max})\ (S - S_{min})^2}{(S_{opt} - S_{min})\Big(\big((S_{opt} - S_{min})(S_N - S_{opt})\big) - \big((S_{opt} - S_{max})(S_{opt} + S_{min} - 2S)\big)\Big)}\right] \quad (17)$$

Regarding the nutrient yield of bacteria, the ones proposed by the ASM models (Henze et al., 2000) were considered a good approximation, and they are summarized in Table 3.

3.4.4. Dissolved oxygen

During the day, microalgae produce oxygen through photosynthesis, which is partially consumed for algal and bacteria respiration. At the same time, dissolved oxygen can be desorbed to the atmosphere according to two different phenomena: (i) natural mass transfer from the culture to the atmosphere in the reactor channels and paddlewheel; (ii) oxygen release and consecutive reduction of the culture dissolved oxygen thanks to the bubbling of air in the reactor sump. The two phenomena are represented by two different mass transfer coefficients K_{la} (equal to 1.0 and 110 h^{-1} respectively) and Henry law as described in (18):

$$m_{O_2} = Kla_i\left(H_{O_2}P_{O_2} - S_{O_2}\right) \quad (18)$$

4. Model parameters

4.1. Calibration procedure

Figure 2 represents the calibration strategy adopted. The experimental dataset used to calibrate the model parameters was selected to include data from different seasons, such as summer, winter, and intermediate seasons (28/04-15/05, 9/08-15/08, 1/11-15/11). In total, the calibration days chosen were 41 (20% of the total amount of data). In this way, it was possible to address the parameters by accounting for various climatic conditions. The final set of parameters was chosen once the objective function described in (19) was minimized.

$$Obj = \sum \frac{\sum(y_{sim} - y_{exp})^2}{\sigma_{exp}} \quad (19)$$

where y_{sim} is the model output, y_{exp} the experimental data and σ_{exp} is the experimental data standard deviation. The experimental data used for the model calibration regarded X_{tot}, S_{NH4}, S_{PO4}, S_{NO3}, S_{BSMO}, S_{O2} where X_{tot} was defined as the sum of X_{alg}, X_{nit} and X_{het} and evaluated experimentally as the total dry weight. The model calibration was carried out using Scipy library in Python and “Nelder-Mead” algorithm which is a robust algorithm mainly used for solving unconstrained optimization problems (Gao and Han, 2012). The list of calibrated parameters with their corresponding values is presented in

Table 6.

4.2. Sensitivity analysis

Table 7 presents the findings of a sensitivity analysis that examined all biological and process parameters together with the associated standard deviation. In this analysis, each parameter was individually variated by +/-20% from its nominal value, and the percentage error (20) between the nominal parameter value (y_{nom}) and the variated parameter value (y_{var}) was evaluated.

$$\%\ err = \frac{\sum|y_{nom} - y_{var}|}{\sum y_{var}} * 100 \quad (20)$$

Results indicate that the most sensible parameters are the ones for microalgae growth rate as a function of light (I_{av}, K_a, n), the maximum growth rates of all the organisms ($\mu_{max,alg}$, $\mu_{max,nit}$, $\mu_{max,het}$) and the nutrient yield of NH_4^+ and NO_3^- ($Y_{NH4,alg}$, $Y_{NO3,nit}$, $Y_{NH4,nit}$). Additionally, the cardinal parameters (T_{max}, T_{min}, T_{opt}) of temperature and pH (pH_{max}, pH_{min}, pH_{opt}) show to be highly sensitive. Given their significant impact on the final prediction, these parameters should be carefully selected based on the biological system analysed and the climatic conditions. Notably, only a few of the nutrient yields were deemed relevant to model error.

4.3. Parameters uncertainty and error propagation

Once the most sensible parameters have been identified, it was possible to calculate the model variance and the confidence interval (Denis Dochain, 2001). From the sensitivity analysis, it was possible to define a sensitivity matrix as (21), which collects the functions of the given output y by variating the parameter p_j.

$$S = \left[\frac{\delta y}{\delta p_1} ; \frac{\delta y}{\delta p_2} ; \dots ; \frac{\delta y}{\delta p_j}\right] \quad (21)$$

The standard deviation of the parameter can be calculated as (22), where C_{ij} is the covariance matrix and p_j is the associated parameter:

$$\vartheta_j^2 = p_j\sqrt{C_{j,j}} \quad (22)$$

The covariance matrix is the inverse of the Fisher information matrix (23), defined as the variance of the score function (Fujita et al., n.d.).

$$F = C^{-1} \quad (23)$$

And it can be calculated starting from the sensitivity analysis according to (24):

$$F = S^T Q^{-1} S \quad (24)$$

where Q is the array of the measured standard deviation.

Once the covariance of the parameter has been evaluated, it was possible to estimate the model error propagation of the output variable y at the given instant time t as (25):

$$\sigma_y(t) = \sqrt{\sum_{i=1}^{m} S_i(t)^2 \, \vartheta_{p_j}^2} \quad (25)$$

The model confidence interval at 95% has been calculated on the model output as (26):

$$[y_i - 1.95\sigma_y \; ; \; y_i + 1.95\sigma_y] \quad (26)$$

5. Model validation

The model prediction accuracy has been evaluated by calculating the normalized squared root error (NRMSE) and Theil's inequality coefficient (TIC) (H. Theil. et al., 1959), as described in (26), (27). Results are reported in Table 8, it is important to note that when the TIC is lower than 0.3, it is possible to consider a good agreement between the experimental data and the model predictions. Additionally, Figure 3 to Figure 5 represent the model estimation and the respective experimental data, as described in the next session.

$$NRMSE = \frac{\sqrt{\sum(y_{sim} - y_{exp})^2}}{(y_{exp,max} - y_{exp,min})} \quad (26)$$

$$TIC = \frac{\sqrt{\sum(y_{sim} - y_{exp})^2}}{\sum y_{sim}^2 + \sum y_{exp}^2} \quad (27)$$

Overall, it is possible to affirm that the model can accurately reproduce the biological system. The ABACO-2 model is remarkably accurate for describing the total biomass concentration and the nutrient concentration evolution (NRMSE between 0.14 and 0.23, TIC between 0.16 and 0.24). Additionally, the model accurately can trace the dissolved oxygen in the culture (NRMSE= 0.14, TIC=0.21).

6. Discussion

6.1. Simulation results

Although microalgae-bacteria consortia are considered a promising technology for wastewater treatment, they still address several challenges. An accurate microalgae-bacteria model is a powerful tool to overcome the bottlenecks of this technology (Aparicio et al., 2023). The ABACO-2 model aims to act as a tool for robust and accurate prediction of the evolution of biomass concentration in a microalgae-bacteria system, and, therefore, to differentiate between the evolution of both populations in the face of operational and environmental conditions. Figure 3A represents the evolution of the total biomass concentration from 15th May to 15th November. The dots represent the experimental data while the model is shown with a solid line, and the shading is the model confidence interval at 95%. Total biomass is mean the sum of the contributions of algae and bacteria that can be approximated to the biomass experimentally evaluated through the dry weight method. The results showed that the model reproduces the trend of the experimental data, with a NRMSE=0.21 and TIC=0.16 (Table 8). The concentration of heterotrophic and nitrifying bacteria over the study period is shown in Figure 3B. According to the simulations, heterotrophic bacteria exhibit higher concentrations than nitrifying bacteria as they vary between 0 and 80 $g_{het}•m^{-3}$, whereas nitrifying bacteria range from 0 to 10 $g_{nit}•m^{-3}$. Regarding heterotrophic bacteria, the strong fluctuations observed could be explained by the large variability in the COD concentration in the influent (100 – 600 $gO_2•m^{-3}$). This variability arises from the use of two different types of water sources, one from the University and the other from the city, with the latter typically containing a higher organic matter content.The concentration over the months of the nitrifying bacteria was lower, considering their slower maximum growth rate compared to the one of heterotrophic bacteria. Results show that the concentration of nitrifying bacteria increased from October to November. This increase may be due to a reduction in the aeration rate in this specific period, which decreased from 200 $L•min^{-1}$ (set-point in normal operations) to 50 $L•min^{-1}$. During that months, the dissolved oxygen concentration increased in the culture, as the aeration was insufficient to remove it efficiently. Previous studies have shown that dissolved oxygen concentration strongly influences the growth of microalgae, as it has an inhibitory effect on photosynthetic activity (Rossi et al., 2020a). Thus, by decreasing the concentration of microalgae, nitrifying activity is favoured, as both populations compete for the N-NH_4^+ present in the medium. Previous authors suggested that competition for N-NH_4^+ is the most

513 frequently negative interaction between microalgae and AOB (Aparicio et al., 2022b). The microalgal
514 biomass concentration is represented in Figure 3C. Algal productivity is primarily influenced by
515 variations in light and temperature throughout the seasons (Muñoz and Bernard, 2021). During
516 spring, the biomass concentration is approximately 0.7 $g_{alg} \cdot L^{-1}$, while in summer it can reach higher
517 values of up to 1.5 $g_{alg} \cdot L^{-1}$. However, during the colder seasons, it decreases to 0.3 $g_{alg} \cdot L^{-1}$. Overall,
518 the model effectively captures the evolution of biomass concentration, highlighting the prevalence of
519 algae biomass compared to bacterial biomass within the culture. Although there is a lack of
520 experimental data on bacterial concentration, this outcome remains reasonable, supported by
521 analysis conducted in previous studies on similar systems (Sánchez Zurano et al., 2020).

522 Figure 4 represents the PO_4^{3-} NO_3^-, BSMO and NH_4^+ concentration in $g \cdot m^{-3}$ respectively. In Figure
523 4A it is shown that the phosphate concentration in the culture can vary between 10 and 60 $g_{PO4} \cdot m^{-3}$.
524 The uptake of this component depends only on the activity of microalgae, given that the influence of
525 bacteria can be considered negligible. In previous studies, it has been demonstrated that the
526 consumption of phosphate is efficient, but not sufficient to lower it to a concentration below the
527 minimum required for the waster discharge (Nordio et al., 2023). Figure 4B represents the NO_3^-
528 concentration, that remained constant from May to October, however, from October to November, it
529 was observed an increase in the NO_3^- concentration, mainly generated during the nitrification process
530 by nitrifiers. The concentration of this compound can vary greatly (between 0 and 300 $g_{NO3} \cdot m^{-3}$)
531 depending on the activity of the nitrifying bacteria, which, as already explained, was enhanced at the
532 end of the study. Nitrate increase and accumulation in the system can be considered one of the main
533 challenges in microalgae-bacteria-based systems. A decrease in microalgae activity leads to an
534 increase in nitrifying activity, which results in the accumulation of nitrate in the medium. The nitrate
535 generated must be consumed by the microalgae. However, as long as ammonium is available in the
536 medium, it will not be consumed or will be consumed slowly, in breach of discharge regulations.
537 Therefore, ensuring correct microalgae activity is essential to achieve treated water at the end of the
538 process. Regarding the organic matter, its degradation is due to the activity of the heterotrophic
539 bacteria and it can be present with a concentration of up to 250 $g_{O2} \cdot m^{-3}$ in the culture (Figure 4C).
540 Finally, in Figure 4D there is the evolution of the ammonium concentration. It is possible to observe

541 that, despite the high NH_4^+ concentration entering the system with the wastewater, in the outlet its
542 concentration is mostly lower than 60 $g_{NH4}•m^{-3}$, meaning that microalgae and nitrifiers can uptake
543 this nutrient with a high efficiency. The peak generated by the simulation is mainly due to the high
544 concentration of this compound entering the system during the dilution/harvesting process at a
545 specific time of the day.

546 Concluding, Figure 5 represents the simulation of the dissolved oxygen in the culture. Specifically,
547 Figure 5A shows the experimental and simulated values of dissolved oxygen concentration along
548 the entire study period, while Figure 5B shows the representation of the dissolved oxygen
549 concentration in a shorter period. The concentration of dissolved oxygen can reach a high
550 concentration during the day due to the microalgal photosynthesis (up to 25 $mg_{O2}•L^{-1}$), while it
551 decreases to anoxic conditions during the night due to the couple effect the algae and bacteria
552 respiration.

553 The results obtained show that the evolution of nutrients in the system together with the simulated
554 biomass concentration agree with those obtained in the experimental data, demonstrating the
555 usefulness of ABACO-2 in microalgae-based systems for wastewater treatment, and its potential on
556 an industrial scale.

557 6.2. Case study: evaluating microalgae-bacteria consortia as function of the operational
558 conditions

559 Studying the populations living in wastewater systems treated with microalgae poses a significant
560 challenge, primarily because there are no fully validated protocols to effectively differentiate between
561 bacterial and microalgal communities. The primary method for assessing biomass in raceway
562 reactors is dry weight, encompassing contributions from both algae and bacteria. Separating them
563 remains challenging yet significant, as their ratios impact various process outcomes, such as
564 biomass quality and water remediation efficiency. Some methods, like successive filtrations based
565 on cell size differences, have been explored, though they often result in a notable presence of
566 bacteria clinging to microalgae due to cell aggregation (Sánchez-Zurano et al., 2020). Alternative
567 methods, including flow cytometry techniques (FCM), prove valuable in assessing the relative

568 composition of mixed microorganism populations, encompassing both prokaryotes and eukaryotes.
569 This approach discriminates between groups by analyzing intrinsic characteristics of individual cells,
570 such as size, complexity, and autofluorescence. Additionally, molecular identification techniques like
571 amplification of 16S and 18S rDNA sequences serve to evaluate microbial community structure
572 (Barreiro-Vescovo et al., 2021). Alongside these methods, photo-respirometry, based on traditional
573 respirometry, has been employed to discern population differences (Rossi et al., 2018). However,
574 these methods lack a direct correlation in biomass concentration ($g \cdot L^{-1}$), which is more
575 straightforward to interpret.

576 In this context, mathematical models offer a useful tool of indirectly study how the balance between
577 populations evolves. Operational conditions, notably cultivation height, dilution/harvesting strategy,
578 and oxygen removal capacity, exibihit a substantial influence. This section presents a case study
579 employing the ABACO-2 model to assess how the proportion between algae and bacteria shifts
580 based on the operational conditions. Simulations have been carried out using the same solar
581 radiation and temperature registered for the validation of the model. On the contrary, the inlet values
582 of nutrient concentration have been maintained constant (as a average values measured in the
583 wastewater medium) in order to avoid their influence in the evaluation of the process conditions (180
584 $mg \cdot L^{-1}$ NH_4^+, 30 $mg \cdot L^{-1}$ PO_4^{3-}, 80 $mg \cdot L^{-1}$ BSMO, 3.4 $mg \cdot L^{-1}$ NO_3^-).

585 ### 6.2.1. Culture height

586 The cultivation height is one of the fundamental parameters to consider when operating raceway-
587 type reactors as it significantly influences the penetrative capacity of light within the cultivation. It has
588 been demonstrated that light reaches the cells only in the first three centimeters of culture, while the
589 rest remains in a state of darkness due to an effect of autoshading, and, therefore, photosynthetically
590 inactive. Furthermore, light penetration depends on other factors, such as the extinction coefficient
591 (K_a), which can vary from cultivation to cultivation and depends on the property of microalgae to
592 scatter the received light (Barceló-Villalobos et al., 2019).

593 In general, facilities that aim to treat large quantities of water prefer to operate at a rather high culture
594 height, around 30 cm. However, this could be a disadvantage in terms of producing high-quality

biomass, as the dark zone favors the growth of bacterial populations over phototrophic ones. Figure 6 A,B and C show the populations varying with cultivation height among the seasons (summer, spring and autumn). As expected, at 8 cm, the algal productivity is favored at the expense of the amount of treated water, with the maximum concentration reached in spring as it is the period when the maximum irradiance is reached (Figure 6A). The possibility of being able to increase productivity by reducing the culture height has already been studied through the development of new reactors called "thin layers" that operate at around 2 cm; they have also been tested for treating wastewater in previous studies (Morillas-España et al., 2021a). On the contrary, microalgal concentration decreases as much as the culture height increases, mitigating the effects related to the different seasons, in favour of the proliferation of the bacterial population (Figure 6B,C). This is particularly evident in the case of nitrifiers. An increased water depth and greater availability of ammonium, owing to a reduced uptake capacity by microalgae, enable an increase in their activity. Previous works demonstrated that the depth of the culture has a striking effect on the composition of the microalgae-bacteria consortia, specially in relative abundance of nitrifiers (Figure 6C). Remarkably, at an 8 cm depth where algae activity is more significant, ammonium consumption mainly occurs within the algae population, resulting in minimal involvement of nitrifying bacteria. Conversely, variations in cultivation height appear to have little effect on the concentration of heterotrophic bacteria (Figure 6B). This is because they do not compete with microalgae for nutrient uptake like nitrifying bacteria; their primary substrate is organic carbon.

In conclusion, the choice of the optimal culture height is of relevance and its regulation mainly depend on the specific goals of the remediation process. These goals may involve achieving high-quality, productive biomass or ensuring efficient water treatment on a larger scale. While a lower culture height is generally recommended to facilitate light penetration, further studies should be carried to avoid heat accumulation and the cellular death. Moreover, it's essential to recognize that significantly increasing the culture depth could enhance the activity of nitrifying bacteria and lead to the accumulation of NO_3^- within the reactor. Based on the outcomes of this simulation study, a culture height of 15 cm appears as a good compromise between treated water quantity, productivity, and balance between algal and bacterial populations.

6.2.2. Dilution/harvesting rate

The harvesting/dilution factor is defined as the reverse of the hydraulic retention time (in day^{-1}) and it plays a crucial role in microalgae industrial production. When deciding on the best approach to adopt, key considerations include the optimal dilution rate and its application method - whether through continuous or semi-continuous mode. In the first case, dilution occurs gradually over the 12 hours of daylight, while in the latter, both dilution and harvesting take place at specific moments of the day. Figure 6 D, E and F illustrate how varying the dilution rate can impact the productivity and composition of algal-bacterial populations, assuming to operate the reactor in a semi-continous mode. The optimal dilution rates for algae range between 0.15 to 0.2 day^{-1}, exceeding these rates leads to a significant decrease in productivity (Figure 6D). This finding is consistent with previous research in similar raceway reactors, which suggested a fixed optimal dilution rate of 0.2 day^{-1} throughout the year (Morillas-España et al., 2020). Concerning the bacterial population, it is evident that nitrifying activity decreases significantly beyond a dilution rate of 0.2 day^{-1}. This phenomenon, known as "culture washout," indicates that the growth rate of nitrifying bacteria lags behind the dilution rate, potentially affecting process effectiveness (Figure 6F). Conversely, a contrasting positive impact is observed on heterotrophic bacteria with increased dilution rates (Figure 6E). This could be attributed to their rapid growth rate and the enhanced organic matter influx, promoting proliferation.

In summary, the simulations presented in this study underscore the critical importance of selecting the optimal dilution factor for the efficient operation of raceway reactors. Traditionally, dilution factors are determined experimentally through batchs, which establish the maximum growth rate and consequently the dilution rate. Alternatively, some studies have suggested comparing reactors at different dilutions operated in parallel. While these methods are effective, they can be laborious and time-consuming. Furthermore, conventional laboratory techniques primarily evaluate productivity in terms of dry weight without delving into the dynamics of the populations involved. Therefore, our research demonstrates that a simulation-based approach offers a viable alternative for identifying the most effective dilution and harvesting strategies.

6.2.3. Air desorption

The concentration of oxygen in a microalgae culture is crucial in biological systems. When oxygen levels surpass air saturation, they can induce inhibitory effects due to the diffusion of dissolved oxygen through microalgae membranes, resulting in oxidative stress on the cells. This inhibitory impact becomes more pronounced with prolonged exposure to elevated oxygen levels (Antonino Baez and Joseph Shiloach, 2014). Microalgae, as photosynthetic organisms, generate oxygen while consuming carbon dioxide, leading to its accumulation in the culture. Studies, such as the one conducted by Rossi et al. in 2020, have shown that excessive oxygen accumulation in cultures can hinder microalgal cell growth (Rossi et al., 2020b). However, there is a scarcity of research assessing how oxygen levels actually influence productivity on a large scale. The prevailing assumption is that oxygen is naturally removed through channels or within the paddlewheel zone. Nonetheless, our experimental data presented herein emphasize the necessity of air injection to reduce oxygen levels in the reactor.

Figure 6G, H, and I illustrate the simulation results in scenarios both without air injection and with a Kla equal to 110 h^{-1}. Once again, it is evident that forced air input is advantageous in promoting algal population production compared to bacterial populations (Figure 6G). Specifically, when air is not removed, microalgal concentration drastically decreases by 65%, underscoring the significance of air injection in the reactor to lower dissolved oxygen levels. Concerning the bacteria, it's notable that air injection predominantly affects nitrifying population, with heterotrophic ones being less affected. Heterotrophic batteries exhibit a slight decrease in concentration when air isn't injected. Conversely, nitrifying batteries show significant growth when oxygen isn't removed from the reactor using compressed air. These results align with the model validation discussed earlier and may offer an explanation for occasional NO^-_3 accumulations in cultures. As previously explained, validation data indicated increased nitrification activity when air injection was reduced from 200 L min^{-1} to 50 L min^{-1}, unfavoring algal growth but favoring nitrification. These simulations confirm this trend, although further experimental studies are needed for confirmation.

In conclusion, these simulations reaffirm the critical significance of oxygen removal from the reactor, not only for enhancing productivity but also for ensuring effective water remediation.

Conclusions

ABACO-2 is a comprehensive model for microalgae-bacteria consortia in wastewater systems. The model was calibrated and validated in a pilot-scale wastewater treatment reactor, exposed to environmental changes and fed with real urban wastewater (with daily changes in the concentration of nitrogen, phosphorus and organic matter), over a long period (May-November). The model allowed to predict the biomass, dissolved oxygen and nutrient concentration evolution with high accuracy. Overall, the use of the ABACO-2 model's relative simplicity allows for good predictions while offering advantages in terms of understanding, practicality, efficiency, and versatility. Concluding, the ABACO-2 model can be considered a useful biological model for the description of algae-bacteria in wastewater systems. In order to increase the robusteness, in the future it will be necessary to carry out additional validation studies in several data set (accounting for different climatologies and wastewater types) and in higher industrial scales.

Credit authorship contribution statement

R. Nordio: Investigation, Formal Analysis, Validation, Software, Data Curation, Visualization, Writing – Original Draft; **E. Rodríguez-Miranda**: Investigation, Formal Analysis, Validation, Software, Data Curation, Writing – Original Draft; **F. Casagli:** Formal analysis, Validation**; A. Sanchez-Zurano:** Investigation, Writing – Original Draft; **J. L. Guzmán**: Conceptualization, Supervision, Writing - Review & Editing, Funding Acquisition; **G. Acien**: Conceptualization, Supervision, Writing - Review & Editing, Funding Acquisition.

Acknowledgements

This research was funded by the H2020 Research and Innovation Programme under the Marie Sklodowska-Curie grant agreement (project: Digitalgaesation, 955520) and by the H2020 Research and Innovation Framework Programme (projects: PRODIGIO, 101007006; REALM, 101060991). Also, this work was supported by the Spanish Ministry of Science and Innovation (project:

HYCO2BIO, PID2020-112709RB-C21). All the authors would like to thank the Institute for Agricultural and Fisheries Research and Training (IFAPA).

References

Abdel-Raouf, N., Al-Homaidan, A.A., Ibraheem, I.B.M., 2012. Microalgae and wastewater treatment. Saudi J Biol Sci. https://doi.org/10.1016/j.sjbs.2012.04.005

Acién, F.G., Ferná Ndez, J.M., Molina-Grima, E., 2014. Economics of Microalgae Biomass Production.

Angelakis, A.N., Gikas, P., 2014. Water reuse: Overview of current practices and trends in the world with emphasis on EU states, Water Utility Journal.

Antonino Baez, Joseph Shiloach, 2014. Effect of elevated oxygen concentration on bacteria, yeasts, and cells propagated for production of biological compounds. Microb Cell Fact 13.

Aparicio, S., González-Camejo, J., Seco, A., Borrás, L., Robles, Á., Ferrer, J., 2023. Integrated microalgae-bacteria modelling: application to an outdoor membrane photobioreactor (MPBR). Science of the Total Environment 884. https://doi.org/10.1016/j.scitotenv.2023.163669

Aparicio, S., Robles, Á., Ferrer, J., Seco, A., Borrás Falomir, L., 2022a. Assessing and modeling nitrite inhibition in microalgae-bacteria consortia for wastewater treatment by means of photo-respirometric and chlorophyll fluorescence techniques. Science of the Total Environment 808. https://doi.org/10.1016/j.scitotenv.2021.152128

Aparicio, S., Robles, Á., Ferrer, J., Seco, A., Borrás Falomir, L., 2022b. Assessing and modeling nitrite inhibition in microalgae-bacteria consortia for wastewater treatment by means of photo-respirometric and chlorophyll fluorescence techniques. Science of the Total Environment 808. https://doi.org/10.1016/j.scitotenv.2021.152128

Barceló-Villalobos, M., Fernández-del Olmo, P., Guzmán, J.L., Fernández-Sevilla, J.M., Acién Fernández, F.G., 2019. Evaluation of photosynthetic light integration by microalgae in a pilot-scale raceway reactor. Bioresour Technol 280, 404–411. https://doi.org/10.1016/j.biortech.2019.02.032

Barreiro-Vescovo, S., González-Fernández, C., de Godos, I., 2021. Characterization of communities in a microalgae-bacteria system treating domestic wastewater reveals dominance of phototrophic and pigmented bacteria. Algal Res 59. https://doi.org/10.1016/j.algal.2021.102447

Bernard, O., Rémond, B., 2012. Validation of a simple model accounting for light and temperature effect on microalgal growth. Bioresour Technol 123, 520–527. https://doi.org/10.1016/j.biortech.2012.07.022

Buhr, H., O., Miller, S., B., 1983. A dynamic model of the high-rate algal-bacterial wastewater treatment pond. Water Research 17, 29–37.

Casagli, F., Zuccaro, G., Bernard, O., Steyer, J.P., Ficara, E., 2021. ALBA: A comprehensive growth model to optimize algae-bacteria wastewater treatment in raceway ponds. Water Res 190. https://doi.org/10.1016/j.watres.2020.116734

Costache, T.A., Gabriel Acien Fernandez, F., Morales, M.M., Fernández-Sevilla, J.M., Stamatin, I., Molina, E., 2013. Comprehensive model of microalgae photosynthesis rate as a function of culture conditions in photobioreactors. Appl Microbiol Biotechnol 97, 7627–7637. https://doi.org/10.1007/s00253-013-5035-2

741 Council Directive of May 1991 concerning urban waste water treatment, 1991.

742 Darvehei, P., Bahri, P.A., Moheimani, N.R., 2018. Model development for the growth of microalgae: A
743 review. Renewable and Sustainable Energy Reviews. https://doi.org/10.1016/j.rser.2018.08.027

744 Denis Dochain, 2001. Bioprocees control , in: Denis Dochain (Ed.), . Wiley-ISTE Series, pp. 52–56.

745 Droop, M.R., 1970. Vitamin B 12 and marine ecology. Continous culture as an approach to nutritional
746 kinetics. Journal of the Marine Biological Association of the United Kingdom 48, 629–636.

747 Fernández Sevilla, J.M., Molina Grima, E., Perez Parra, J., Acién Fernández, F.G., Magán Cañadas, J.J.,
748 Friedi, T., 2006. New species of microalgae and its application for animal and human
749 consumption and in the production of carotenoids. WO 2006/087405.

750 Fujita, K., Okada, K., Katahira, K., n.d. The Fisher information matrix: A tutorial for calculation for
751 decision making models.

752 Gao, F., Han, L., 2012. Implementing the Nelder-Mead simplex algorithm with adaptive parameters.
753 Comput Optim Appl 51, 259–277. https://doi.org/10.1007/s10589-010-9329-3

754 Grima, E.M., Camacho, F.G., Pérez, J.A.S., Sevilla, J.M.F., Fernández, F.G.A., Gómez, A.C., 1994. A
755 mathematical model of microalgal growth in light-limited chemostat culture. Journal of Chemical
756 Technology & Biotechnology 61, 167–173. https://doi.org/10.1002/jctb.280610212

757 Grivalský, T., Ranglová, K., da Câmara Manoel, J.A., Lakatos, G.E., Lhotský, R., Masojídek, J., 2019.
758 Development of thin-layer cascades for microalgae cultivation: milestones (review). Folia
759 Microbiol (Praha). https://doi.org/10.1007/s12223-019-00739-7

760 Henze, Mogens., Gujer, Willi., Mino, Takashi., Van Loosdrecht, Mark., 2000. Activated sludge models
761 ASM1, ASM2, ASM2d and ASM3. IWA Pub.

762 Ippoliti, D., Gómez, C., del Mar Morales-Amaral, M., Pistocchi, R., Fernández-Sevilla, J.M., Acién, F.G.,
763 2016. Modeling of photosynthesis and respiration rate for Isochrysis galbana (T-Iso) and its
764 influence on the production of this strain. Bioresour Technol 203, 71–79.
765 https://doi.org/10.1016/j.biortech.2015.12.050

766 Lee, E., Jalalizadeh, M., Zhang, Q., 2015. Growth kinetic models for microalgae cultivation: A review.
767 Algal Res. https://doi.org/10.1016/j.algal.2015.10.004

768 Masojídek, J., Gómez-Serrano, C., Ranglová, K., Cicchi, B., Encinas Bogeat, Á., Câmara Manoel, J.A.,
769 Sanches Zurano, A., Silva Benavides, A.M., Barceló-Villalobos, M., Robles Carnero, V.A., Ördög,
770 V., Gómez Pinchetti, J.L., Vörös, L., Arbib, Z., Rogalla, F., Torzillo, G., Lopez Figueroa, F., Acién-
771 Fernándéz, F.G., 2022. Photosynthesis Monitoring in Microalgae Cultures Grown on Municipal
772 Wastewater as a Nutrient Source in Large-Scale Outdoor Bioreactors. Biology (Basel) 11.
773 https://doi.org/10.3390/biology11101380

774 Mohd Udaiyappan, A.F., Abu Hasan, H., Takriff, M.S., Sheikh Abdullah, S.R., 2017. A review of the
775 potentials, challenges and current status of microalgae biomass applications in industrial
776 wastewater treatment. Journal of Water Process Engineering.
777 https://doi.org/10.1016/j.jwpe.2017.09.006

778 Monod, J., 1949. THE GROWTH OF BACTERIAL CULTURES.

779 Morillas-España, A., Lafarga, T., Acién-Fernández, F.G., Gómez-Serrano, C., González-López, C.V.,
780 2021a. Annual production of microalgae in wastewater using pilot-scale thin-layer cascade
781 photobioreactors. J Appl Phycol 33, 3861–3871. https://doi.org/10.1007/s10811-021-02565-2

782 Morillas-España, A., Lafarga, T., Gómez-Serrano, C., Acién-Fernández, F.G., González-López, C.V., 2020.
783 Year-long production of Scenedesmus almeriensis in pilot-scale raceway and thin-layer cascade
784 photobioreactors. Algal Res 51. https://doi.org/10.1016/j.algal.2020.102069

785 Morillas-España, A., Lafarga, T., Sánchez-Zurano, A., Gabriel Acién-Fernández, F., Rodríguez-Miranda,
786 E., Gómez-Serrano, C., Cynthia, &, González-López, V., 2021b. Year-long evaluation of microalgae
787 production in wastewater using pilot-scale raceway photobioreactors: Assessment of biomass
788 productivity and nutrient recovery capacity.

789 Muñoz, I.L., Bernard, O., 2021. Modeling the influence of temperature, light intensity and oxygen
790 concentration on microalgal growth rate. Processes 9. https://doi.org/10.3390/pr9030496

791 Muñoz, R., Guieysse, B., 2006. Algal-bacterial processes for the treatment of hazardous contaminants:
792 A review. Water Res. https://doi.org/10.1016/j.watres.2006.06.011

793 Ncr, (, Clinton, J., 1999. CRISP-DM 1.0 Step-by-step data mining guide. DaimlerChrysler.

794 Nordio, R., Delgado, F.J., Sánchez-Zurano, A., Hernandez, J.G., Rodríguez-Miranda, E., Guzmán, J.L.,
795 Lafarga, T., Acién, G., 2023. Long-term assessment of the nutrient recovery capacity and biomass
796 productivity of Scenedesmus almeriensis in raceway reactors using unprocessed urban
797 wastewater. Bioresour Technol 369. https://doi.org/10.1016/j.biortech.2022.128374

798 Pasztor I., Thury P., Pulai J., 2009. Chemical oxygen demand fractions of municipal wastewater for
799 modeling of wastewater treatment. International Journal of Enviornmental Science and
800 Technology 6, 51–56.

801 Posadas, E., Morales, M. del M., Gomez, C., Acién, F.G., Muñoz, R., 2015. Influence of pH and CO2
802 source on the performance of microalgae-based secondary domestic wastewater treatment in
803 outdoors pilot raceways. Chemical Engineering Journal 265, 239–248.
804 https://doi.org/10.1016/j.cej.2014.12.059

805 Rossi, S., Bellucci, M., Marazzi, F., Mezzanotte, V., Ficara, E., 2018. Activity assessment of microalgal-
806 bacterial consortia based on respirometric tests. Water Science and Technology 78, 207–215.
807 https://doi.org/10.2166/wst.2018.078

808 Rossi, S., Casagli, F., Mantovani, M., Mezzanotte, V., Ficara, E., 2020a. Selection of photosynthesis and
809 respiration models to assess the effect of environmental conditions on mixed microalgae
810 consortia grown on wastewater. Bioresour Technol 305.
811 https://doi.org/10.1016/j.biortech.2020.122995

812 Rossi, S., Casagli, F., Mantovani, M., Mezzanotte, V., Ficara, E., 2020b. Selection of photosynthesis and
813 respiration models to assess the effect of environmental conditions on mixed microalgae
814 consortia grown on wastewater. Bioresour Technol 305.
815 https://doi.org/10.1016/j.biortech.2020.122995

816 Sánchez Zurano, A., Garrido Cárdenas, J.A., Gómez Serrano, C., Morales Amaral, M., Acién-Fernández,
817 F.G., Fernández Sevilla, J.M., Molina Grima, E., 2020. Year-long assessment of a pilot-scale thin-
818 layer reactor for microalgae wastewater treatment. Variation in the microalgae-bacteria
819 consortium and the impact of environmental conditions. Algal Res 50.
820 https://doi.org/10.1016/j.algal.2020.101983

Sánchez Zurano, A., Gómez Serrano, C., Acién-Fernández, F.G., Fernández-Sevilla, J.M., Molina-Grima, E., 2021. Modeling of photosynthesis and respiration rate for microalgae–bacteria consortia. Biotechnol Bioeng 118, 952–962. https://doi.org/10.1002/bit.27625

Sánchez-Zurano, A., Gómez-Serrano, C., Acién-Fernández, F.G., Fernández-Sevilla, J.M., Molina-Grima, E., 2020. A novel photo-respirometry method to characterize consortia in microalgae-related wastewater treatment processes. Algal Res 47. https://doi.org/10.1016/j.algal.2020.101858

Sánchez-zurano, A., Rodríguez-miranda, E., Guzmán, J.L., Acién-fernández, F.G., Fernández-sevilla, J.M., Grima, E.M., 2021. Abaco: A new model of microalgae-bacteria consortia for biological treatment of wastewaters. Applied Sciences (Switzerland) 11, 1–24. https://doi.org/10.3390/app11030998

Solimeno, A., García, J., 2017. Microalgae-bacteria models evolution: From microalgae steady-state to integrated microalgae-bacteria wastewater treatment models – A comparative review. Science of the Total Environment. https://doi.org/10.1016/j.scitotenv.2017.07.114

Solimeno, A., Gómez-Serrano, C., Acién, F.G., 2019. BIO_ALGAE 2: improved model of microalgae and bacteria consortia for wastewater treatment. Environmental Science and Pollution Research 26, 25855–25868. https://doi.org/10.1007/s11356-019-05824-5

Solovchenko, A.E., Ismagulova, T.T., Lukyanov, A.A., Vasilieva, S.G., Konyukhov, I. V., Pogosyan, S.I., Lobakova, E.S., Gorelova, O.A., 2019. Luxury phosphorus uptake in microalgae. J Appl Phycol. https://doi.org/10.1007/s10811-019-01831-8

Strosser, P., Dworak, T., Andrés Garzon Delvaux, P., Berglund, M., Schmidt, G., Mysiak, J., Kossida, M., Iacovides, I., Ashton, V., Seiz Puyuelo, R., De Paoli, G., Stanley, K., 2012. Gap Analysis of the Water Scarcity and Droughts Policy in the EU Final Report Gap Analysis of the Water Scarcity and Droughts Policy in the EU European Commission.

Zambrano, J., Krustok, I., Nehrenheim, E., Carlsson, B., 2016. A simple model for algae-bacteria interaction in photo-bioreactors.

Zurano, A.S., Serrano, C.G., Acién-Fernández, F.G., Fernández-Sevilla, J.M., Molina-Grima, E., 2021. Modelling of photosynthesis, respiration, and nutrient yield coefficients in Scenedemus almeriensis culture as a function of nitrogen and phosphorus. Appl Microbiol Biotechnol 105, 7487–7503. https://doi.org/10.1007/s00253-021-11484-8

Tables

Table 1.- ABACO-2 model process rates

n.	Process	Process rate [g•m^{-3}•day^{-1}]
1	Microalgae growth on NH_4	$\mu_{max,alg} \cdot \mu(I_{av}) \cdot \overline{\mu(T)} \cdot \overline{\mu(pH)} \cdot \overline{\mu(O_2)_{alg}} \cdot \overline{\mu(N-NH_4)} \cdot \overline{\mu(P-PO_4)} \cdot X_{alg}$
2	Microalgae growth on NO_3	$\mu_{max,alg} \cdot \mu(I_{av}) \cdot \overline{\mu(T)} \cdot \overline{\mu(pH)} \cdot \overline{\mu(O_2)_{alg}} \cdot \overline{\mu(N-NO_3)} \cdot \overline{\mu(P-PO_4)} \cdot \left(1-\overline{\mu(N-NH_4)}\right) \cdot X_{alg}$
3	Microalgae decay	$m \cdot X_{alg}$
4	Nitrifying bacteria growth	$\mu_{max,nit} \cdot \overline{\mu_{nit}(T)} \cdot \overline{\mu_{nit}(pH)} \cdot \overline{\mu_{nit}(O_2)} \cdot \overline{\mu_{nit}(N-NH_4)} \cdot X_{nit}$
5	Nitrifying bacteria decay	$\theta_{nit} \cdot m_{nit} \cdot X_{nit}$
6	Heterotrophic bacteria growth	$\mu_{max,het} \cdot \overline{\mu_{het}(T)} \cdot \overline{\mu_{het}(pH)} \cdot \overline{\mu_{het}(O_2)} \cdot \overline{\mu_{het}(N-NH_4)} \cdot \overline{\mu_{het}(BSMO)} \cdot X_{het}$
7	Heterotrophic bacteria decay	$\theta_{het} \cdot m_{het} \cdot X_{het}$

Table 2.- ABACO-2 yields matrix

	Component → i	S_{NH4}	S_{NO3}	S_{PO4}	S_{BSMO}	S_{O2}	X_{alg}	X_{nit}	X_{het}
j	Process ↓	[g_{NH4}•m^{-3}]	[g_{NO3}•m^{-3}]	[g_{PO4}•m^{-3}]	[g_{BSMO}•m^{-3}]	[g_{O2}•m^{-3}]	[g_{alg}•m^{-3}]	[g_{nit} •m^{-3}]	[g_{het} •m^{-3}]
1	Microalgae growth on NH_4	$-Y_{NH_4,alg}$		$-Y_{PO_4,alg}$		$+Y_{O2,alg}$	1		
2	Microalgae growth on NO_3		$-Y_{NO_3,alg}$	$-Y_{PO_4,alg}$		$+Y_{O2,alg}$	1		
3	Microalgae decay				$1-f_{alg}$	$-Y_{O2,alg}$	-1		
4	Nitrifying bacteria growth	$-Y_{NH_4,nit}$	$+Y_{NO_3,nit}$			$-Y_{O2,nit}$		1	
5	Nitrifying bacteria decay				$1-f_{bac}$			-1	
6	Heterotrophic bacteria growth	$-Y_{NH_4,het}$			$-Y_{BSMO}$	$-Y_{O2,het}$			1
7	Heterotrophic bacteria decay				$1-f_{bac}$				-1

Table 3.- Stoichiometric coefficients.

Parameter	Value	Units	Source
$Y_{NH_4,nit}$	7.9	$g_{NH_4} \cdot g_{nit}{}^{-1}$	(Henze et al., 2000)
$Y_{NO_3,nit}$	26.7	$g_{NO_3} \cdot g_{nit}{}^{-1}$	(Henze et al., 2000)
$Y_{NH_4,het}$	0.16	$g_{NH_4} \cdot g_{het}{}^{-1}$	(Henze et al., 2000)
Y_{BSMO}	2.3	$g_{BSMO} \cdot g_{het}{}^{-1}$	(Henze et al., 2000)

$Y_{O2,alg}$	1.33	$g_{O_2} \cdot g_{alg}{}^{-1}$	
$Y_{O2,nit}$	12.44	$g_{O_2} \cdot g_{nit}{}^{-1}$	(Henze et al., 2000)
$Y_{O2,het}$	0.4	$g_{O_2} \cdot g_{het}{}^{-1}$	(Henze et al., 2000)
f_{alg}	0.1	–	(Solimeno et al., 2019)
f_{bac}	0.1	–	(Solimeno et al., 2019)
θ_{het}	1.07	$°C$	(Casagli et al., 2021)
θ_{nit}	1.1	$°C$	(Casagli et al., 2021)

Table 4.- Microalgae kinetic parameters.

Parameter	Value	Units	Source
Microalgae kinetic parameters			
I_K	168	$\mu E \cdot m^{-2} \cdot s^{-1}$	(Sánchez Zurano et al., 2021)
n	1.7	–	(Sánchez Zurano et al., 2021)
K_a	0.08	$m^2 g^{-1}$	This study
I_{K_r}	134	$\mu E \cdot m^{-2} \cdot s^{-1}$	(Sánchez Zurano et al., 2021)
n_r	1.4	–	(Sánchez Zurano et al., 2021)
$T_{min,alg}$	-10	$°C$	(Casagli et al., 2021)
$T_{max,alg}$	38	$°C$	(Casagli et al., 2021)
$T_{opt,alg}$	20	$°C$	(Casagli et al., 2021)
$pH_{min,alg}$	1.8	–	(Sánchez Zurano et al., 2021)
$pH_{max,alg}$	12.9	–	(Sánchez Zurano et al., 2021)
$pH_{opt,alg}$	8.5	–	(Sánchez Zurano et al., 2021)
$S_{O_2,max}$	22.68	$g_{O_2} \cdot m^{-3}$	(Sánchez Zurano et al., 2021)
z	4.15	–	(Sánchez Zurano et al., 2021)
$K_{S,NH_4,alg}$	1.98	$g_{NH_4} \cdot m^{-3}$	(Zurano et al., 2021)
$K_{i,NH_4,alg}$	734	$g_{NH_4} \cdot m^{-3}$	(Zurano et al., 2021)
$n_{NH_4,alg}$	2	-	(Zurano et al., 2021)

$K_{s,NO_3,alg}$	12.26	$g_{NO_3} \cdot m^{-3}$	(Zurano et al., 2021)
$K_{i,NO_3,alg}$	1713	$g_{NO_3} \cdot m^{-3}$	(Zurano et al., 2021)
$n_{NO_3,alg}$	2	–	(Zurano et al., 2021)
$K_{S,PO_4,alg}$	1.31	$g_{PO_4} \cdot m^{-3}$	(Zurano et al., 2021)
Heterotropic bacteria kinetic parameters			
$T_{min,het}$	-3	$°C$	(Casagli et al., 2021)
$T_{max,het}$	42	$°C$	(Casagli et al., 2021)
$T_{opt,het}$	25	$°C$	(Casagli et al., 2021)
$pH_{min,het}$	6	–	(Sánchez Zurano et al., 2021)
$pH_{max,het}$	12	–	(Sánchez Zurano et al., 2021)
$pH_{opt,het}$	9	–	(Sánchez Zurano et al., 2021)
$K_{s,O_2,het}$	1.98	$g_{O_2} \cdot m^{-3}$	(Sánchez Zurano et al., 2021)
$K_{S,NH_4,het}$	0.64	$g_{NH_4} \cdot m^{-3}$	(Henze et al., 2000)
$K_{S,BSMO,het}$	0.299	$g_{BMSO} \cdot m^{-3}$	(Henze et al., 2000)
Nitrifying bacteria kinetic parameters			
$T_{min,nit}$	-8	$°C$	(Casagli et al., 2021)
$T_{max,nit}$	38	$°C$	(Casagli et al., 2021)
$T_{opt,nit}$	20	$°C$	(Casagli et al., 2021)
$pH_{min,nit}$	2	–	(Sánchez Zurano et al., 2021)
$pH_{max,nit}$	13.4	–	(Sánchez Zurano et al., 2021)
$pH_{opt,nit}$	9	–	(Sánchez Zurano et al., 2021)
$K_{s,O_2,nit}$	1.080	$g_{O_2} \cdot m^{-3}$	(Henze et al., 2000)
$K_{s,O_2,nit}$	104.9	$g_{O_2} \cdot m^{-3}$	(Henze et al., 2000)
$K_{S,NH_4,nit}$	1.28	$g_{NH_4} \cdot m^{-3}$	(Henze et al., 2000)

866

867 Table 5.- Microalgae nutrient yield parameters.

Parameter	Value	Units	Source	Parameter	Value	Units	Source	Parameter	Value	Units	Source
$Y_{NH_4,max}$	0.77	$g_{NH_4} \cdot g_{alg}$	Calibrated	$Y_{NO_3,max}$	0.44	$g_{NO_3} \cdot g_{alg}$	Calibrated	$Y_{PO_4,max}$	0.001	$g_{PO_4} \cdot g_{alg}$	Calibrated
K_{S,NH_4}	32	$g_{NH_4} \cdot m^{-3}$	(Zurano et al., 2021)	K_{S,No_3}	141	$g_{NO_3} \cdot m^{-3}$	(Zurano et al., 2021)	$K_{S,PO_4,}$	10	$g_{PO_4} \cdot m^{-3}$	(Zurano et al., 2021)
t_{NH_4}	2	-		t_{NO_3}	2	-		$t_{PPO_4,}$	2.14	-	
$NH_{4_{max}}$	102	$g_{NH_4} \cdot m^{-3}$		$NO_{3_{max}}$	102	$g_{NO_3} \cdot m^{-3}$		$PO_{4_{max}}$	69	$g_{PO_4} \cdot m^{-3}$	
$NH_{4_{min}}$	12	$g_{NH_4} \cdot m^{-3}$		$NO_{3_{min}}$	12	$g_{NO_3} \cdot m^{-3}$		$PO_{4_{min}}$	6	$g_{PO_4} \cdot m^{-3}$	
$NH_{4_{opt}}$	71	$g_{NH_4} \cdot m^{-3}$		$NO_{3_{opt}}$	71	$g_{NO_3} \cdot m^{-3}$		$PO_{4_{opt}}$	47	$g_{PO_4} \cdot m^{-3}$	

868

869

870 Table 6.- List of calibrated parameters and their corresponding values

Parameter	Description	Value	Units
$\mu_{max,alg}$	Maximum algal growth rate	1.5	day^{-1}
m_{min}	Minimum algal respiration rate	0.1	day^{-1}
m_{max}	Maximum algal respiration rate	0.008	day^{-1}
$\mu_{max,nit}$	Maximum nitrifying bacteria growth rate	0.75	day^{-1}
m_{nit}	Nitrifying bacteria decay	0.05 $\mu_{max,nit}$	day^{-1}
$\mu_{max,het}$	Maximum heterotrophic bacteria growth rate	3.4	day^{-1}
m_{het}	Heterotrophic bacteria decay	0.2 $\mu_{max,het}$	day^{-1}
$Y_{NH_4,max}$	NH_4^+ microalage nutrient yield max	0.6	$g_{NH_4} \cdot g_{alg}{}^{-1}$
$Y_{NO_3,max}$	NO_3^- microalage nutrient yield max	0.1	$g_{NO_3} \cdot g_{alg}{}^{-1}$
$Y_{PO_4,max}$	PO_4^{3-} microalage nutrient yield max	0.004	$g_{PO_4} \cdot g_{alg}{}^{-1}$
Kl_a	O_2 natural mass transfer	0.1	h^{-1}
α	Nutrient assimilation coefficient	1	–

871

872 Table 7.- List of most sensible parameters

Parameter	Units	Nominal value	Standard deviation	Most affected parameters
I_k	$\mu E \cdot m^{-2} \cdot s^{-1}$	168	0.02	$X_{alg}, X_{het}, X_{nit}, S_{NH_4}, S_{NO_3}, S_{PO_4}, S_{BSMO}, S_{O_2}$
K_a	$m^2 g^{-1}$	0.08	1.4E-5	$X_{alg}, X_{het}, X_{nit}, S_{NH_4}, S_{NO_3}, S_{PO_4}, S_{BSMO}, S_{O_2}$
n	–	1.7	1.6E-4	$X_{alg}, X_{het}, X_{nit}, S_{NO_3}, S_{PO_4}, S_{O_2}$
$\mu_{max,alg}$	day^{-1}	1.5	5.38E-4	$X_{alg}, X_{het}, X_{nit}, S_{NH_4}, S_{NO_3}, S_{PO_4}, S_{BSMO}, S_{O_2}$
$\mu_{max,het}$	day^{-1}	3.4	0.0016	X_{het}, S_{BSMO}
$\mu_{max,nit}$	day^{-1}	0.75	0.0004	$X_{nit}, S_{NO_3}, S_{NH_4}$
m_{min}	day^{-1}	0.1	8E-6	$X_{alg}, X_{het}, X_{nit}, S_{NO_3}, S_{BSMO}, S_{O_2}$
m_{nit}	day^{-1}	0.05 $\mu_{max,nit}$	8.34E-5	$X_{het}, X_{nit}, S_{NO3} S_{BSMO},$
m_{het}	day^{-1}	0.2 $\mu_{max,het}$	6.8E-5	$X_{het}, X_{nit}, S_{NO3} S_{BSMO},$
$O_{2,max}$	$mg_{O_2} \cdot l^{-1}$	22.68	0.0011	$X_{alg}, X_{het}, X_{nit}, S_{NO_3}, S_{PO_4}, S_{BSMO}, S_{O_2}$
$Y_{NH_4,max}$	–	0.6	0.001	X_{het}, X_{nit} S_{NH_4}, S_{NO_3}
$Y_{NH_4 nit}$	–	0.4	0.016	X_{nit} , S_{NH_4}
$Y_{NO_3,nit}$	–	26.76	0.11	S_{NO_3}
Cardinal parameters	**Units**	**Opt, max, min**	**Standard deviation**	**Most affected parameters**
T_{alg}	$°C$	38,20,-10	0.0026	$X_{alg}, X_{het}, X_{nit}, S_{NH_4}, S_{NO_3}, S_{PO_4}, S_{BSMO}, S_{O_2}$
pH_{alg}	–	8.5, 12.9, 1.8	0.0032	$X_{alg}, X_{het}, X_{nit}, S_{NH_4}, S_{NO_3}, S_{PO_4}, S_{BSMO}, S_{O_2}$
T_{nit}	$°C$	20,38,-8	0.04	X_{het}, X_{nit} $S_{NH_4}, S_{NO_3}, S_{BSMO}$
pH_{nit}	–	9, 13.4, 2	0.024	X_{het}, X_{nit} $S_{NH_4}, S_{NO_3}, S_{BSMO}$
T_{het}	$°C$	25,42,-3	0.034	X_{het}, $X_{nit}, S_{NO_3}, S_{BSMO}$
pH_{het}	–	9, 12, 6	0.0026	X_{het}, $X_{nit}, S_{NO_3}, S_{BSMO}$

873

874

Table 8.- Validation errors of the ABACO-2 model.

Parameter	NRMSE	TIC
$X_{tot}\ [g \cdot m^{-3}]$	0.21	0.16
$S_{NH_4}\ [g \cdot m^{-3}]$	0.22	0.55
$S_{NO_3}\ [g \cdot m^{-3}]$	0.15	0.21
$S_{PO_4}\ [g \cdot m^{-3}]$	0.23	0.24
$S_{BSMO}\ [g \cdot m^{-3}]$	0.21	0.2
$S_{O_2}\ [g \cdot m^{-3}]$	0.14	0.21

Figures

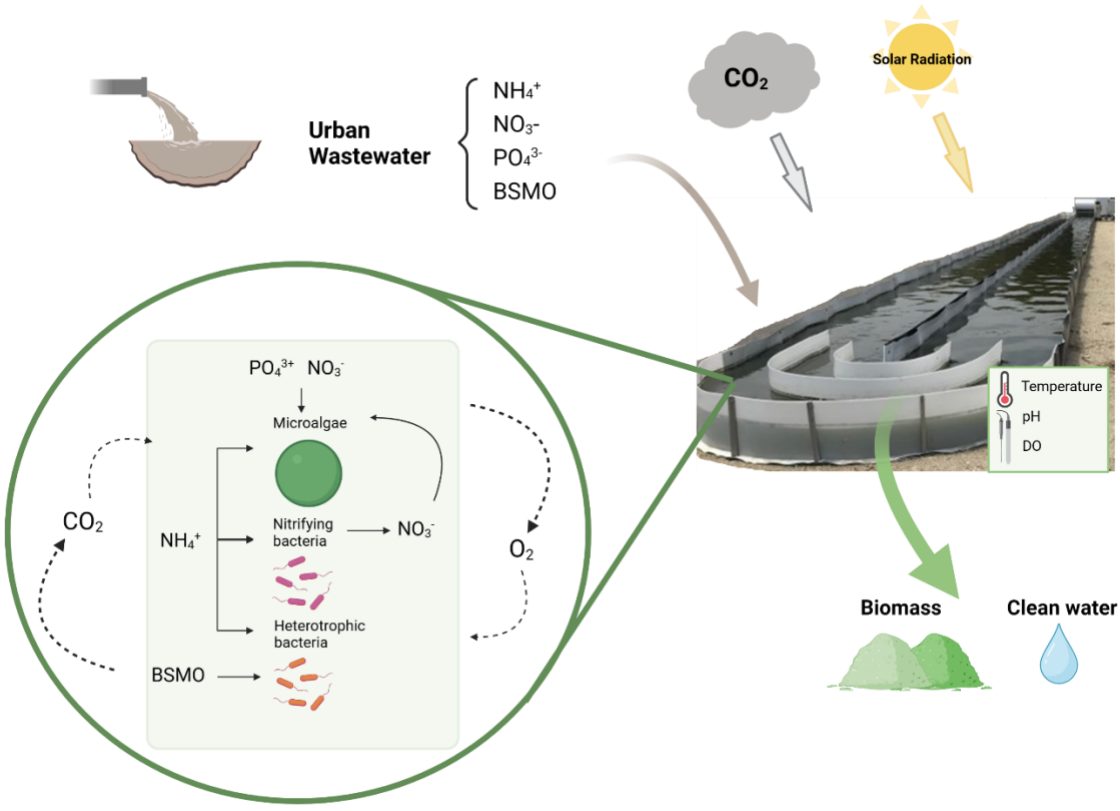

Figure 1.- Schematic description of the biological mechanisms taking in place in microalgae-bacteria wastewater systems.

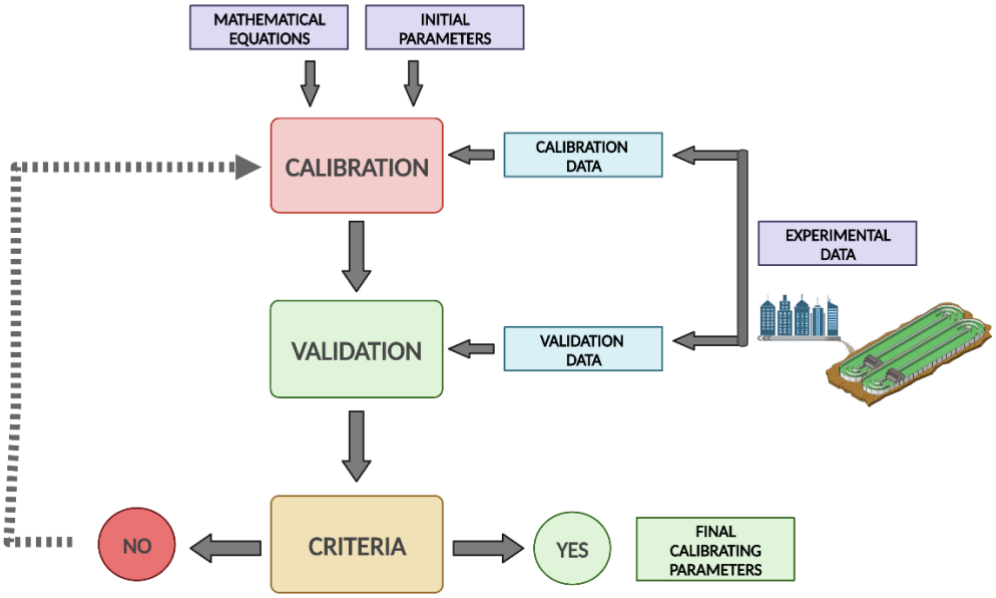

882

883 Figure 2.- Calibration methodology used in the present work.

884

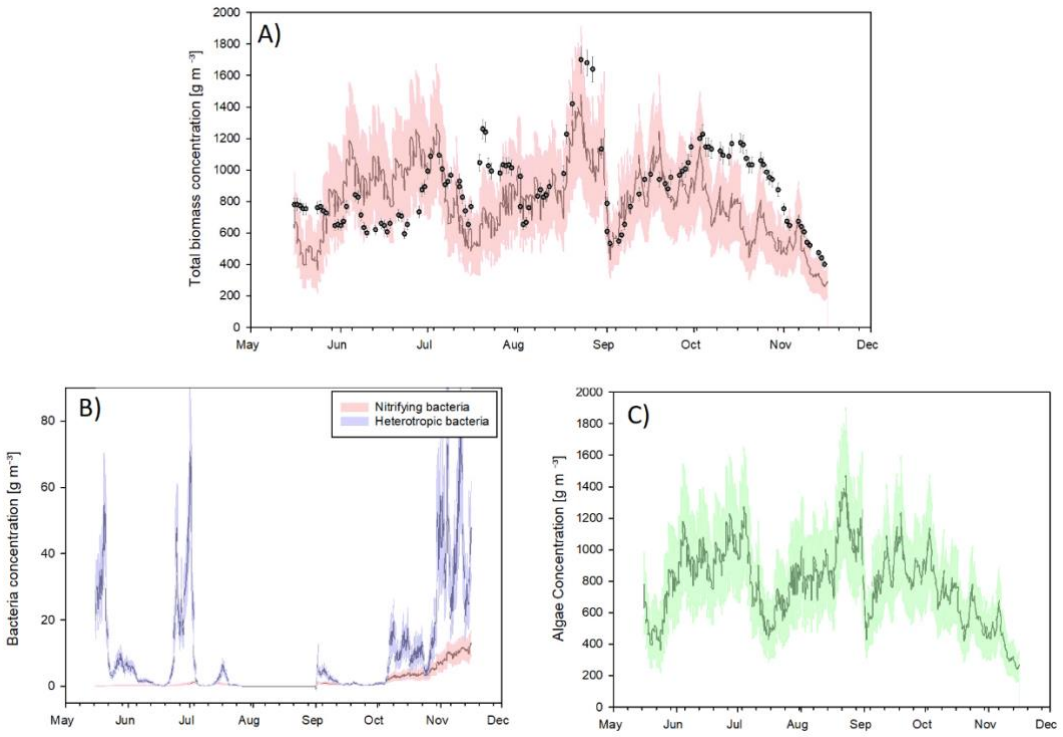

885

886 Figure 3.- Biomass concentration evolution. A) Total biomass concentration (sum of algae and bacteria,
887 simulated (continuous line) and experimental (scatter plot); B) Nitrifying and heterotropic concentration; C)
888 Algae concentration. The model shade is the model confidence interval at 95%.

889

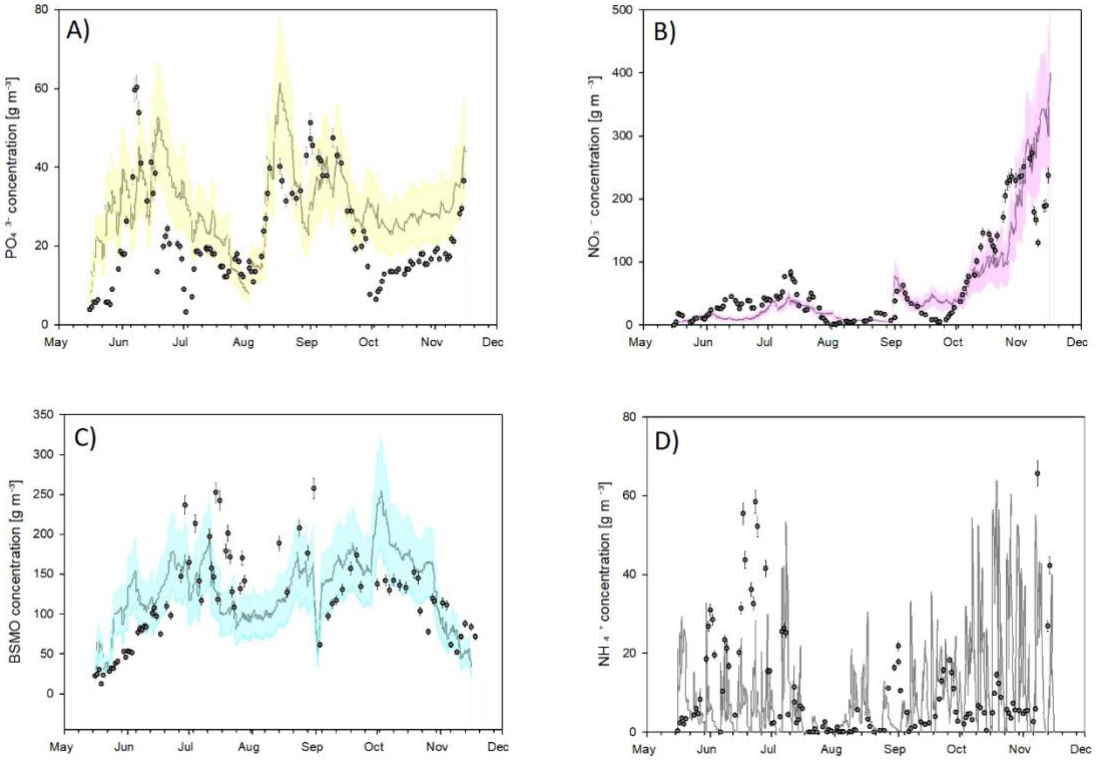

890

891 Figure 4.- Variation of culture nutrients A) PO_4^{3-}, B) NO_3^-, C) NH_4^+ and D) BSMO concentration, in $g \bullet m^{-3}$
892 respectively (experimental, scatter plot; model prediction, continuous line).

893

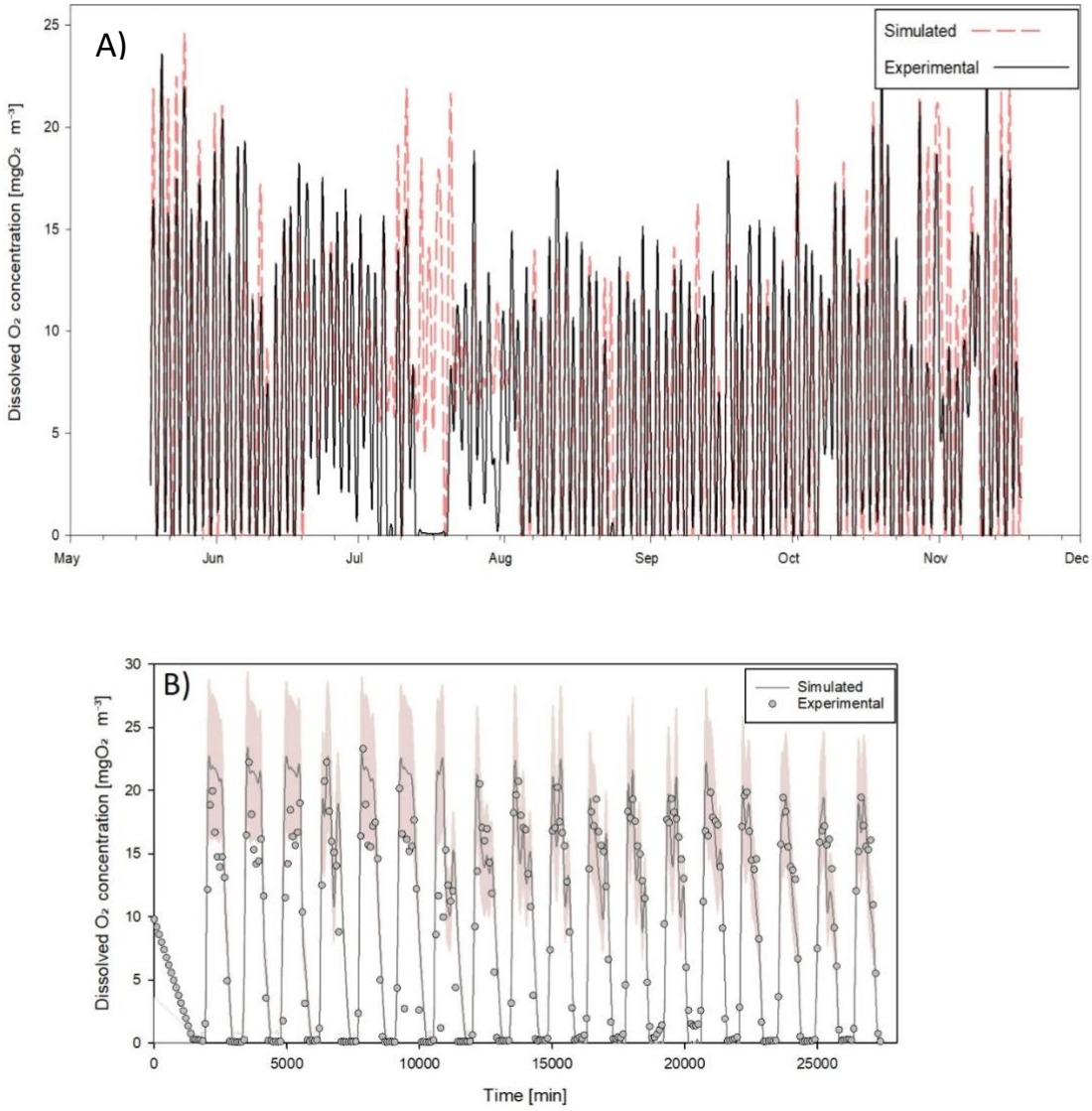

894

895 Figure 5.- Simulation of the dissolved oxygen in the culture. A) Experimental and simulated dissolved
896 oxygen along the entire study period, B) Representation of the oxygen in a shorter period.

897

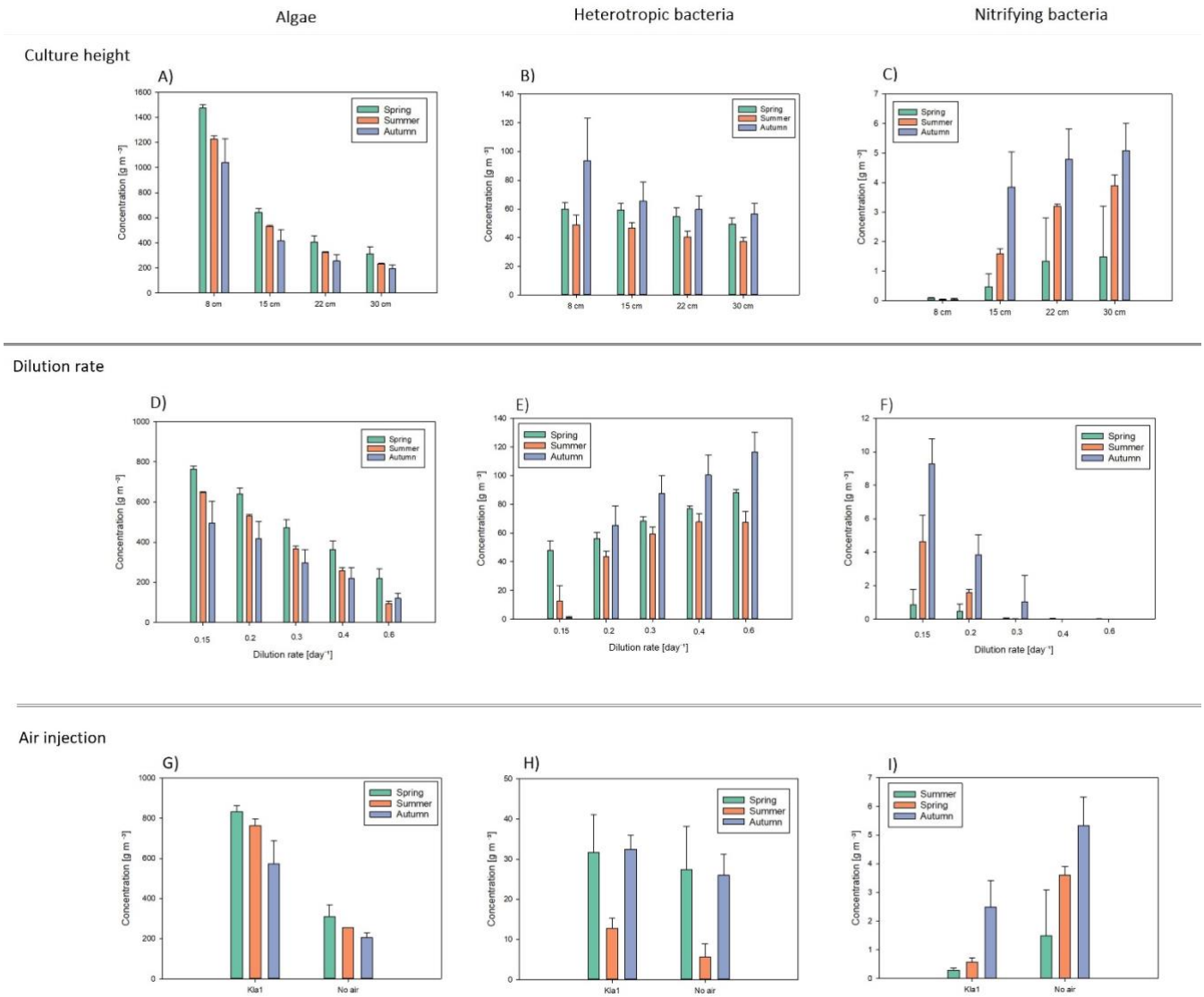

Figure 6: Application of ABACO-2 model in a case-study. Algae, heterotropic and nitrifying bacteria concentration eveolution depending on: A), B), C) culture height; D), E), F) Dilution rate; G), H), I) with or without ijecting air into the system